JOURNAL OF MATERIALS SCIENCE **36** (2001) 1707–1716

Crack spacing statistics and spalling area fractions for indented silica-coated bismaleimide (BMI)

C. MUKHERJEE, E. D. CASE*
Materials Science and Mechanics Department, Michigan State University, East Lansing, MI 48824, USA
E-mail: casee@egr.msu.edu

Indentation loading of thin, continuous silica coatings adhered to Bismaleimide (BMI) polymeric substrates induces a concentric array of cracks in the silica coating. For Vickers indentation, the array consists of diamond-shaped concentric cracks, while Hertzian indentation gives circular concentric cracks. This paper characterizes the indentation-induced crack damage in the coating in terms of: (1) f_s, the area fraction of the coating (within the indentation-cracked region) that spalls off the substrate due to the indentation and (2) the spacing between the cracks in the crack array. For a given indentation crack field, the crack spacing was uniform as a function of radial distance outward from the center of the indentation. One of the key results of this study was that the curing temperature for the coating dramatically affected both the coating spalling area fraction, f_S, and the manner in which the crack spacing changed as a function of the applied indentation load.

1. Introduction

The polymer Bismaleimide (BMI) is a viscous liquid prior to crosslinking, which allows BMI to be processed as easily as an epoxy resin [1, 2]. After curing, BMI's glass transition temperature is approximately 300°C, which is sufficiently high that BMI can be used in a number of high temperature applications of polymeric materials, including in advanced aerospace applications [2–5].

However, BMI is susceptible to attack by organic solvents, moisture, and galvanic corrosion [1]. To enhance BMI's performance, the authors and co-workers [6] have applied thin, continuous silica surface coatings to BMI substrates in an effort to seal out moisture, solvents, and deter galvanic corrosion. In this study and in previous studies of BMI by the authors [6], the silica coating on the BMI substrates were produced by spinning on a preceramic organic liquid and then curing the liquid to obtain an amorphous silica layer.

Vickers indentation can give a rough estimate of the coating's resistance to point contact damage due to material handling and (in the case of aerospace materials) erosion processes such as dust impact and maintenance procedures [7]. For the silica-coated BMI, Vickers indentation damage is manifested as an array of concentric, quasi-diamond shaped cracks, centered at the center of the indentation impression (Fig. 1). For Hertzian indentation, the crack damage field consists of a circular array of cracks (Fig. 2).

Although crack damage is often characterized in terms of crack length, for the periodic array of indentation damage cracks observed for the silica coatings in this study (Figs 1–3), the area spalling fraction, f_S, and the mean crack spacing, μ, are used as measures of the integrated coating damage. The crack field dimensions as a function of the applied indentation load were addressed in earlier studies by the authors and co-workers [6]. An interesting result of this study is that both the spalling fraction and the mean crack spacing can be significantly affected by the curing temperature of the coating. Potentially, adjustments in the curing temperature may be utilized to aid in optimizing coating adhesion for a variety of applications of silica coatings on BMI.

2. Experimental procedure

2.1. Materials

All of the BMI substrates included in this study were formed by reacting two polymeric components, bismaleimidodiphenylmethane (BMPM) and diallyl bisphenol alcohol (DABPA) using a 1 : 1 stoichiometric ratio of BMPM and DABPA. The details of the fabrication of the BMI billets is given elsewhere [1, 2, 6].

High-purity amorphous silica films were fabricated on the BMI specimens using a organically-based preceramic liquid (SilicaFilm^{TM}, Emulsitone Company, Whippany, New Jersey). According to the vendor

* Author to whom all correspondence should be addressed.

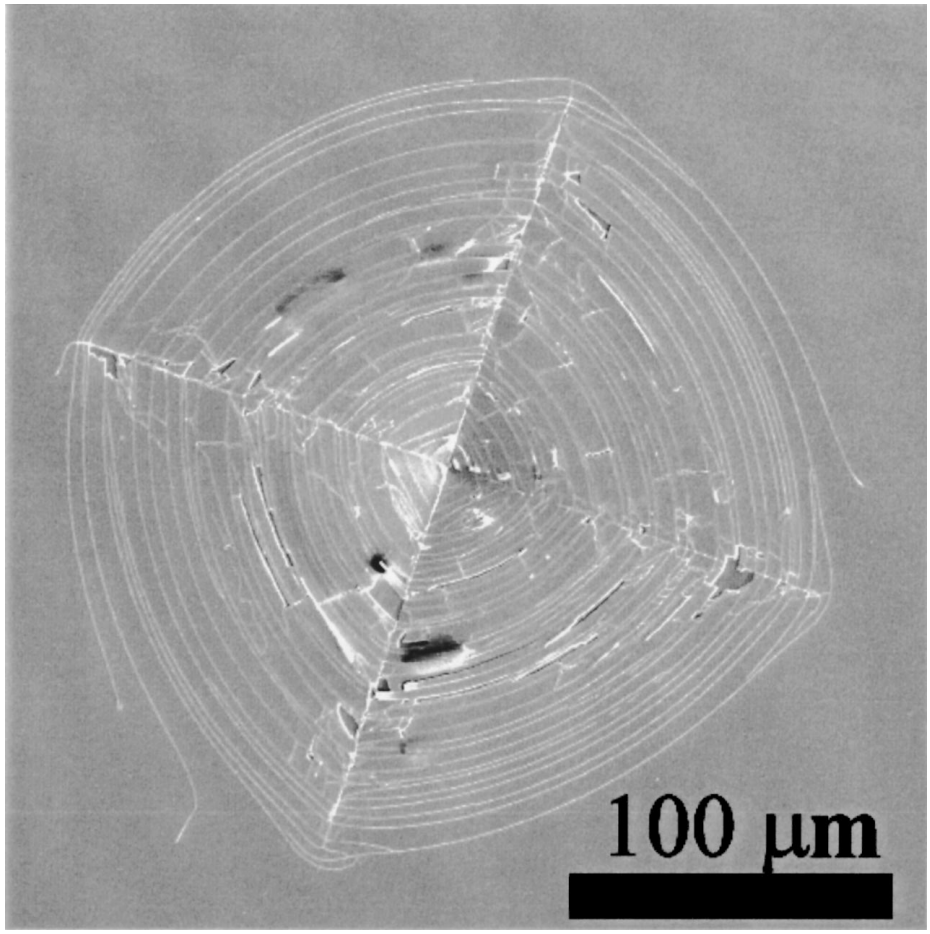

(a)

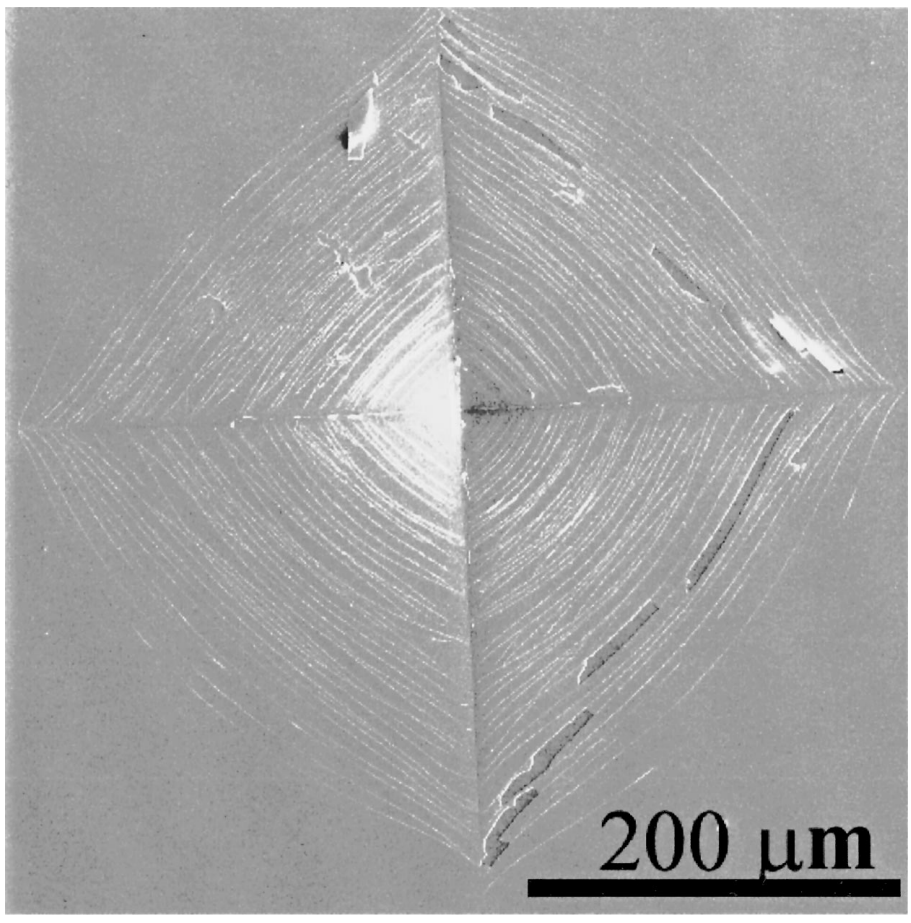

(b)

Figure 1 For 0.15 micron-thick silica coatings on a BMI substrate, crack damage field induced by Vickers indentation at indentation loads of (a) 9.8 N and (b) 49 N. In both micrographs, the coating was cured at 175°C for one hour.

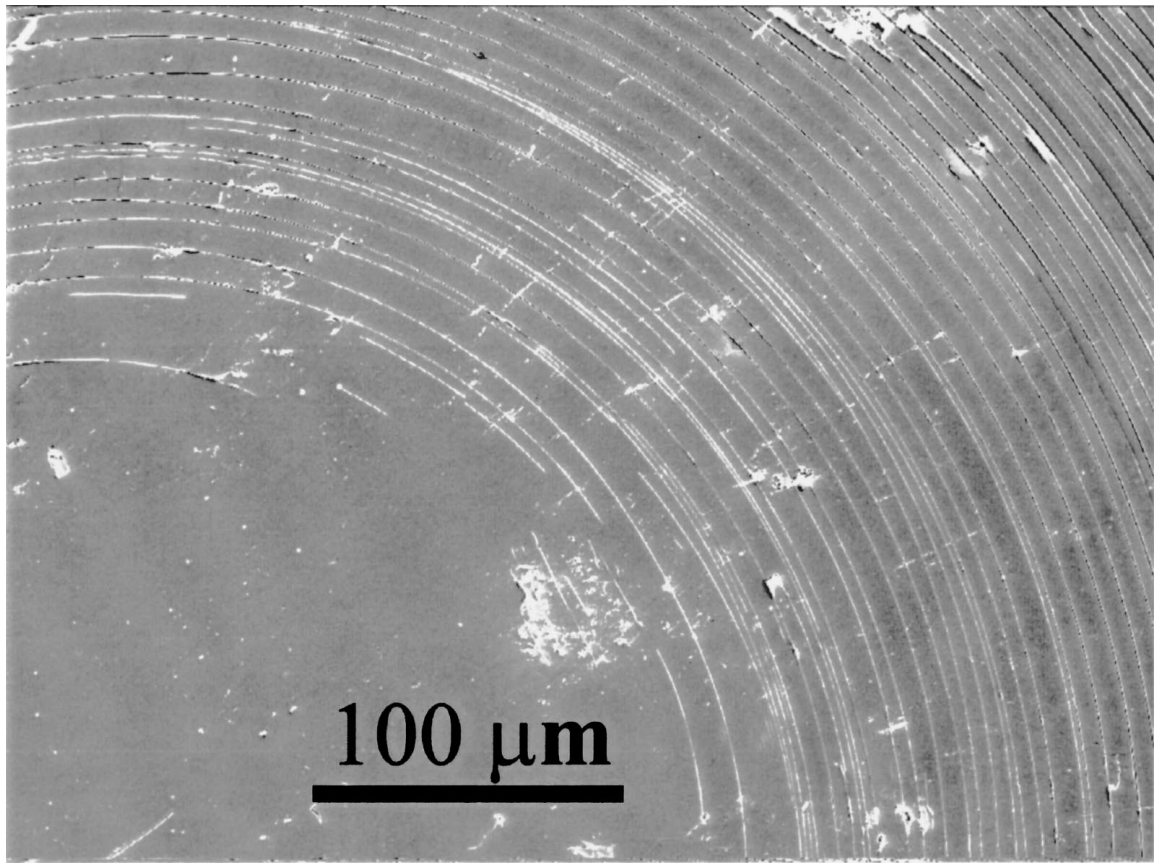

Figure 2 For a 0.15 micron-thick silica coating on a BMI substrate, the crack damage field induced by a Hertzian (spherical ball) indentation at an applied load of 588 N. The coating was cured at 150°C for 20 minutes.

(Emulsitone Company), the metal ion impurity level in the air-cured SilicaFilm^{TM} is less than 1 part per million. (The high purity of the SilicaFilm^{TM} is important in its principal intended use, which is as a passivation layer for integrated circuitry, where the silica layer serves to guard against both abrasion damage and electrical shorting of the fine-line metallized circuitry deposited on the surface of the integrated circuit.) In this study, the SilicaFilm^{TM} provides a convenient method of depositing a variable thickness, high-purity amorphous silica film on the BMI substrate surface. As discussed in next section, the thickness of silica coating is controlled by the spin rate of the substrate, after the SilicaFilm has been applied.

2.2. Specimen preparation

After fabricating the billets, the BMI was cut into 1 cm $\times$ 1 cm $\times$ 0.4 cm specimens using a low speed diamond saw. After sectioning, one of the specimens' 1.0 cm $\times$ 1.0 cm faces was ground with 600-grit abrasive paper followed by polishing with 5 μm, 0.3 μm, and 0.05 μm alumina abrasive powders. The polished BMI substrates then were precured in air at 200°C for one hour.

Using a pipette, approximately five drops of the preceramic silica liquid were applied to the BMI substrate's surface. The specimens were then spun at 4000 rpm for 20 seconds using a high speed substrate spinner. After spinning, the silica-liquid coated specimens were cured in air using one of four curing conditions: (1) 150°C for 20 minutes, (2) 175°C for one hour, (3) 200°C for one hour, and (4) 250°C for one hour. Each of the four curing conditions yielded an amorphous silica film approximately 0.15 micron thick. After curing the coating, two of the specimens which had been cured at 150°C for 20 minutes were abraded using 0.05 μm alumina powder for 45 seconds using a polishing wheel speed of 175 rpm.

2.3. Vickers and Hertzian indentation

For the silica-coated BMI specimens included in this study, crack damage was induced by either Vickers indentation or Hertzian indentation. The Vickers indentations were made using a loading rate of 70 microns/second and loading time of 10 seconds with a semi-macro indenter (Buehler, Lake Bluff, IL). The unabraded specimens were indented at loads varying from 2.94 to 196 N, while the abraded specimens were indented only at loads of 9.8 N and 49 N.

The Hertzian indentations were made using a standard Rockwell indenter (Wilson Mechanical Instrument Co., NY) with a major load of 588 N, a loading time of 10 seconds, and a spherical steel indenter ball 1.5875 mm in diameter. (These loading conditions correspond to the Rockwell F-scale).

2.4. Crack damage characterization

For the crack spacing analysis, micrographs of the Vickers indentation damaged regions were obtained using a Scanning Electron Microscope (SEM) using an accelerating voltage of 20 kV, imaged magnifications

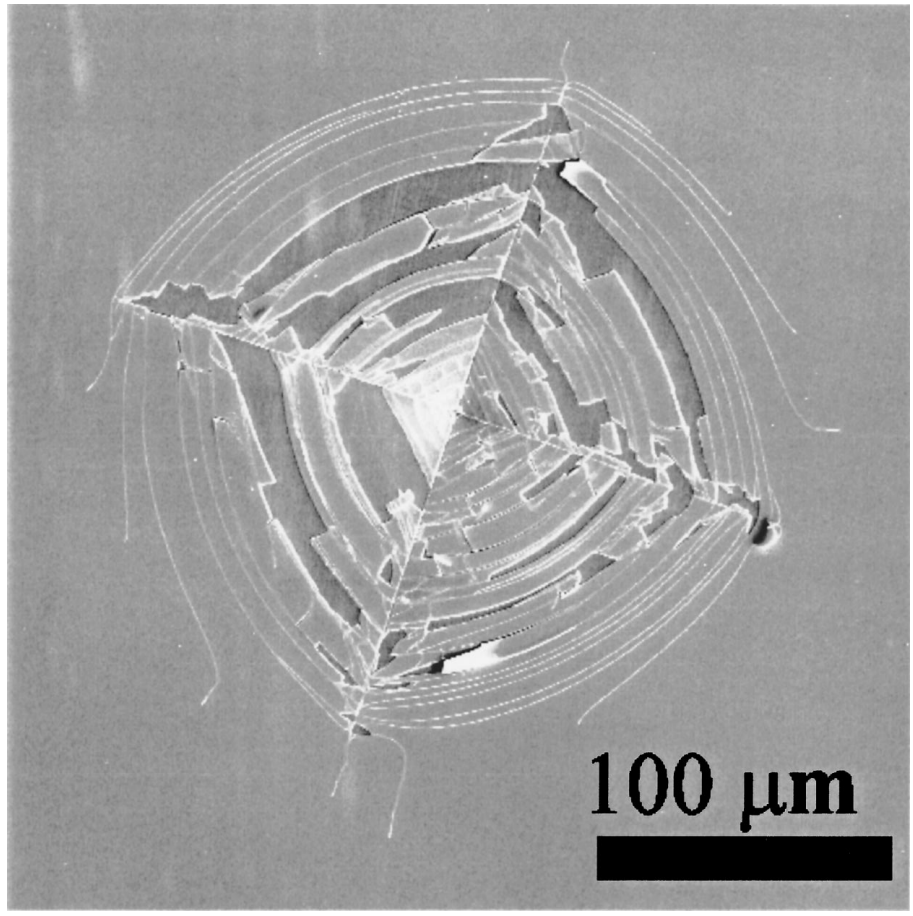

(a)

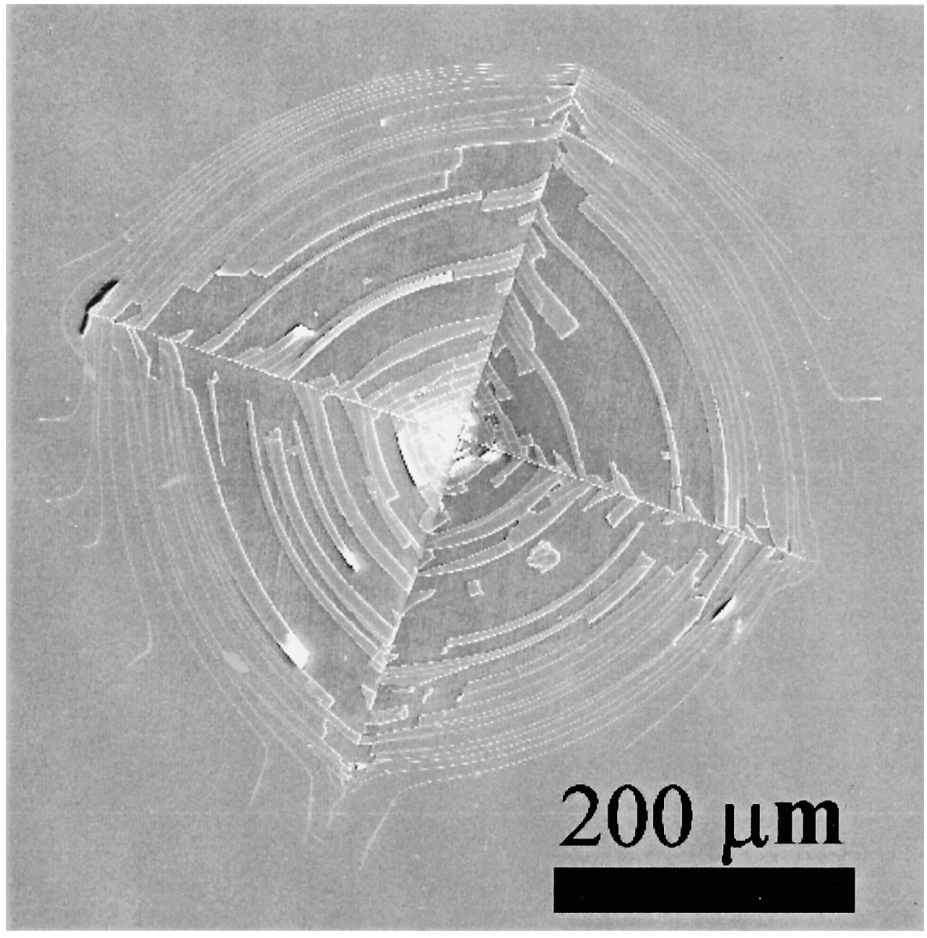

(b)

Figure 3 Micrographs showing the considerable spalling produced by Vickers indentation loading for specimens cured at 150°C for 20 minutes then indented at loads of (a) 9.8 N and (b) 49 N.

of 3000× to 3500×. For the spalling damage measurements, the SEM measurements were performed at magnifications between 300 and 720×, since a wider field of view was needed for the spalling experimentation than for the crack spacing measurements.

All of the individual crack spacings data were measured directly from the SEM micrographs. For the Vickers indentation crack arrays, the measurements were made along the diagonals of the indentation impression. For the Hertzian indentations, the crack length measurements were performed along the radial direction outward from the center of the indentation impression.

The spalled area fraction, f_S, defined as $f_S =$ spalled area/total indented area, was determined using commercial image analysis software. A total of 54 Vickers indentations were analyzed by the image analyzer (9 at each of the 6 indentation loads).

One third of the same set of indentations analyzed by the image analyzer (3 indentations at each of the 6 indentation loads) were re-analyzed by the grid point method (involving counting squares on graph paper directly superimposed on the SEM micrographs). For each of the indentations that were compared, the image analysis and the grid point analysis gave f_S values that agreed to within ±2%, which indicates that the image analysis system did provide rapid and relatively accurate data on the spalling fractions.

3. Results and discussion

3.1. Spalling area fraction for the coating as a function of curing conditions

The silica coatings were cured in air using the following conditions: (1) 150°C for 20 minutes, (2) 175°C for one hour, (3) 200°C for one hour, and (4) 250°C for one hour. While Vickers indentations were made on specimens coated under each of the four curing conditions, Hertzian indentations were made only on coatings cured at 150°C for 20 minutes.

An important trend in the spalling area fractions for the specimens was that curing the coatings at temperatures of 175°C or greater reduced the amount of spalling due to Vickers indentation. In particular, for the silica coated BMI cured at 150°C for 20 minutes (Fig. 3) and 175°C for one hour (Fig. 1), the spalling area fraction f_S, was calculated for nine indentations at each value of load. For the BMI cured at 150°C for 20 minutes, f_S, varied from 0.14 to 0.25 (Fig. 4). However, for the BMI cured at 175°C for one hour, f_S was much smaller, ranging from 0.02 to 0.05 (Fig. 4).

The silica coatings cured at 200°C for one hour and 250°C for one hour yielded f_S values of approximately 0.02 to 0.04 upon Vickers indentation at loads from 2.94 N to 196 N, which is quite similar to the f_S values obtained for the coatings cured at 175°C. However, while the coatings cured at 150°C and 175°C were smooth, continuous, and crack free in the as-cured state, the coatings cured at 200°C and 250°C displayed a network of cracks in the as-cured state (prior to indentation). Due to the cracks present in the coatings prior to indentation, a reduced number of indentation tests were performed for the specimens with coatings cured

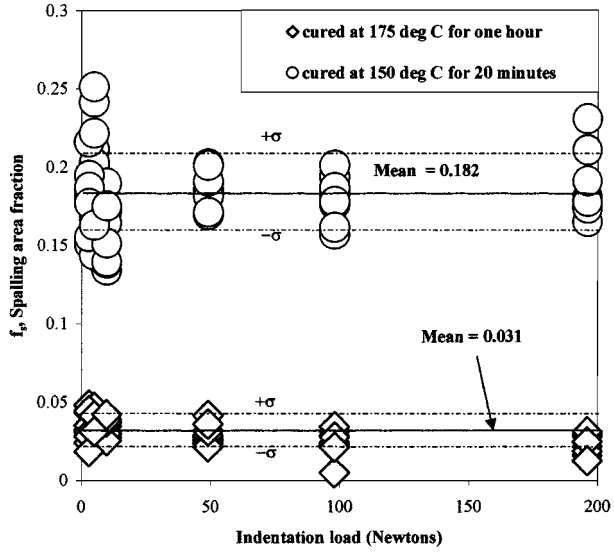

Figure 4 The spalling area fraction f_S, as a function of Vickers indentation load for silica coated BMI cured at 150°C for 20 minutes (open circles) and 175°C for one hour (open triangles).

at 200°C and 250°C, with only two indentations at each load for 2.94 N, 4.9 N, 9.8 N, 49 N, and 98 N, and only one indentation was done at 196 N.

The crack patterns observed in the as-cured specimens for the 200°C and 250°C curing were consistent with cracks induced by thermal expansion differences between the coating and substrate [8]. For example, curing at 200°C produced a network of parallel cracks extending about 3000 to 4000 microns from the specimen edge. On average, approximately one out of 10 cracks in the network coalesced with another crack a distance of roughly of 1000 to 1500 microns from the specimen edge. Based on a total of 71 measurements, the spacing between the parallel cracks was roughly 45.8 microns ±21.3 microns. In addition to the parallel cracks, each of the four corners of the coated specimen face displayed a "mud-flat" pattern of cracks, with a distance between nodes of about 15 to 25 microns. Upon curing at 250°C, the entire surface area of the coated specimens displayed a mud-flat crack pattern. Based on 41 measurements, the average of distance between crack nodes was about 120 microns for the silica coatings cured at 250°C. Therefore, despite the thermal-expansion-mismatch induced crack networks that existed in the silica coatings cured at 200°C and 250°C prior to indentation, the spalling area fraction, f_S, was still comparable to the relatively low values observed for coatings cured at 175°C.

Thus, in this particular coating/substrate system, there is apparently an optimum temperature range (near 175°C) where the silica coatings are (1) crack-free, smooth and continuous after coating and (2) spall relatively little upon indentation by a sharp (Vickers) indenter. The difference in f_S observed for coatings cured at 150°C and those cured at 175°C indicates that the silica film's adhesion to the BMI substrate is a function of curing temperature, which in turn likely stems from temperature-dependent chemical reaction(s) taking place at the silica/BMI interface during curing. However, the details of such interfacial reactions need

to be explored and elucidated in order to understand the basic physical processes involved.

Not unexpectedly, f_S is apparently a function of the indenter tip shape. The value of f_S tends to be lower for the blunt Hertzian (spherical) indenter tips than for the sharp Vickers (square pyramidal) indenter tips. For the silica coatings cured at 150°C for 20 minutes, the Hertzian indentations at 588 N load (Fig. 2) gave f_S values that ranged from 0.06 to 0.08 for a total of six indentations, three each on two specimens, which is considerably lower than the f_S resulting from Vickers indentation on identically-cured coatings. No spherical indentations were done on the coatings cured at temperatures from 175°C to 250°C.

3.2. Crack spacing as a function of radial distance from the indent center

Within a given crack field, the micrographs of the indentation damage indicate that the spacing between adjacent cracks, $d_{i,i+1}$, is relatively uniform over the entire crack field, for both Vickers and Hertzian indentation crack fields (Figs 1 and 2). However, in addition to the qualitative assessment of the crack spacing uniformity obtained by observing the micrographs of crack damage, we also statistically compared the crack spacing data to a uniform distribution (Fig. 5). A uniform distribution $U(a, b)$ has a single value U_O for its entire range over the entire interval (a, b). As an statistical estimator of the value U_O [9, 10], we used the mean crack spacing, μ. Thus, if one assumes a uniform distribution of crack spacings, then μ becomes the predicted or "expected" value of $U(a, b)$, and the actual crack spacing data, $d_{i,i+1}$, are the observed values of $U(a, b)$. The mean crack spacings μ were calculated using

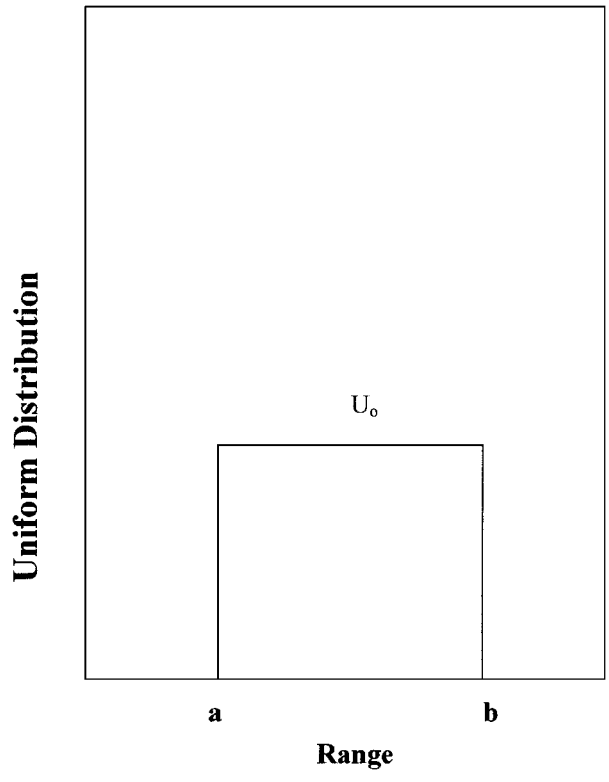

Figure 5 A schematic showing a uniform distribution $U(a, b)$ with the magnitude U_0 over the range (a, b).

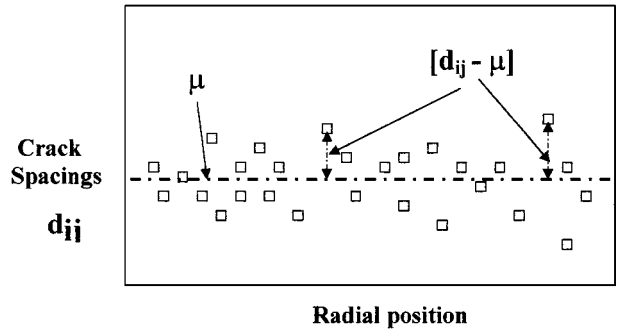

Figure 6 A schematic of the crack spacings versus radial position, showing examples of the differences between the crack spacing d_{ij} and mean crack spacing μ.

$$\mu = \sum_{i=1}^{N} \frac{d_{i,i+1}}{N} \tag{1}$$

where $N =$ the total number of cracks in the interval between the indent center and the outer edge of the indentation-induced crack array. The "residuals", $r_{i,i+1}$, in the statistical analysis are defined as

$$r_{i,i+1} = d_{i,i+1} - \mu \tag{2}$$

and thus the residual $r_{i,i+1}$ values are the differences between the observed and expected values for the distribution (Fig. 6).

An analysis of residuals can be a powerful statistical tool for making inferences about the nature of the distribution itself [11]. In particular, if the magnitude of the residuals $r_{i,i+1}$ are normally distributed, then the typical inference is that $r_{i,i+1}$ reflect random differences in the data (the observed $d_{i,i+1}$ values) with respect to the expected value (here, the mean crack spacing, μ).

The normality of the distribution of the residuals $r_{i,i+1}$, was tested via an order statistics study, in which the set of residuals $r_{i,i+1}$ for a given indentation were arranged in ascending order and numbered from 1 through $N - 1$, where $N - 1$ was the total number of crack spacings in a given data set with N cracks [12]. Using MS Excel software, the ordered residuals were plotted on a normal probability axis against the expected order statistic values, S_I, where S_I is defined by $S_I = (I - 3/8)/(N + 1/4)$ for $I = 1$ to N [12]. In these coordinates (Fig. 7), a straight line corresponds to a normal distribution. For the normal probability plots of the residuals (Fig. 7), the coefficient of determination, R^2, values ranged from 0.904 to 0.986 indicating that the residuals follow a Gaussian distribution [13]. The residuals being normally distributed in turn means that there is a random scatter in crack spacings $d_{i,i+1}$ about the mean μ. In other words, for the individual crack damage fields induced by Vickers or Hertzian indentation, the crack spacing is apparently uniform.

3.3. Mean crack spacing as a function of load, abrasion, and curing conditions

3.3.1. Mean crack spacing measurements

In addition to determining the mean crack spacing, μ, for individual indentation damage fields, the trend in mean crack spacing as a function of load, coating abrasion, and curing conditions was investigated for a total

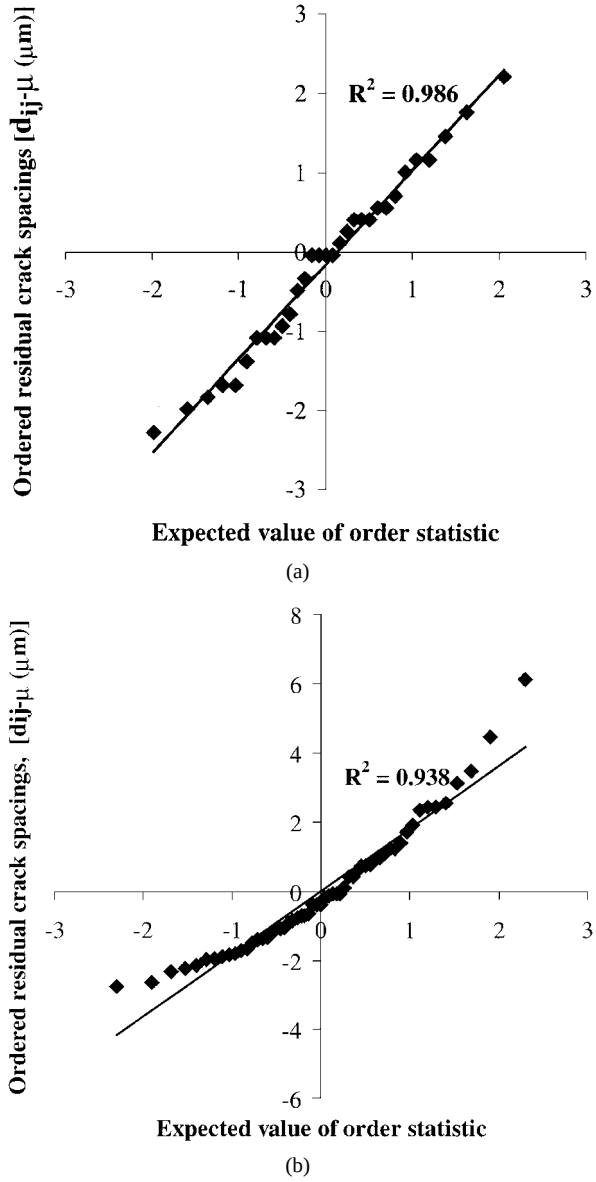

Figure 7 The residual crack spacings versus the expected value of the order statistic [12] for silica coatings cured at 150°C and indented at 49 N for (a) a surface-coating ($R^2 = 0.986$) and (b) an unabraded coating (0.938).

of eighty-four Vickers indentation crack fields and six Hertzian indentation crack fields.

For the unabraded coatings cured at 150°C for 20 minutes, thirty-six Vickers indents were made, six each for each of the six values of indentation load (2.94 N to 196 N). The mean crack spacings, μ, varied from 4.3 microns to 5.0 microns. For the specimens having abraded coatings (which were also cured at 150°C for 20 minutes), six Vickers indentations each were made at loads of 9.8 N and 49 N, which resulted in mean crack spacings μ of 4.3 microns and 4.7 microns, respectively. The overall mean value for both the unabraded and abraded specimens was 4.6 microns, over the entire range of Vickers indentation load from 2.94 N to 196 N (Fig. 8). For the six Hertzian indentation (three indentations on each of two specimens), the mean crack spacing was 4.6 μm, which also is very similar to the mean crack spacing for the Vickers indentations on both the unabraded and abraded silica coatings.

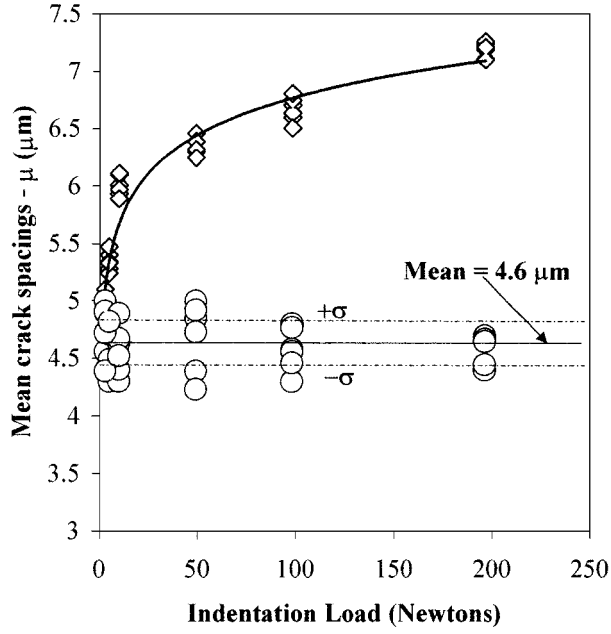

Figure 8 The mean crack spacings versus as a function of indentation load for silica coatings cured at 150°C for 20 minutes (open circles) and 175°C for one hour (open triangles).

The applied indentation loads for the combined data set (Rockwell and Vickers indentations together) span a factor of 200 in load (from 2.94 N to 588 N). For the Vickers indentation work alone, the applied indentation load ranged from a minimum of 2.94 N to a maximum of 196 N (a factor of about 67). Furthermore, this work encompasses different indenter tip materials (diamond for the Vickers and hardened steel for the Rockwell), as well as differing indenter tip shapes (square-pyramid "sharp" indenter tip for the Vickers, and a spherical tip for the Rockwell). Thus, for the coatings cured at 150°C in air for 20 minutes, the mean crack spacing is remarkably independent of load, indenter tip material, and indenter tip shape, and the details of the surface flaw population.

In contrast to the coatings cured at 150°C for 20 minutes, coatings cured at 175°C showed a dependence of the mean crack spacings on applied Vickers indentation load (Fig. 8). At low loads (2.96 N), mean crack spacings for the coatings cured at both 150°C and 175°C were each approximately 4.7 μm. As the applied load increased, the mean crack spacing remained relatively constant for both the unabraded and abraded coatings cured at 150°C for 20 minutes (Fig. 8). However, for the coatings cured at 175°C for one hour, the crack spacing increased monotonically to 7.1 μm for indentation load of 196 N, which is 47% greater than the crack spacing produced at a similar load for coatings cured at 150°C (Fig. 8). An empirical relationship that describes the normalized mean crack length as a function of load is discussed in the next section.

3.3.2. An empirical relationship for crack spacing as a function of load

Although the mean crack spacings for the coatings cured at 150°C and 175°C showed different dependencies upon the applied indentation load (Fig. 8), both sets of crack spacing data are described by a single

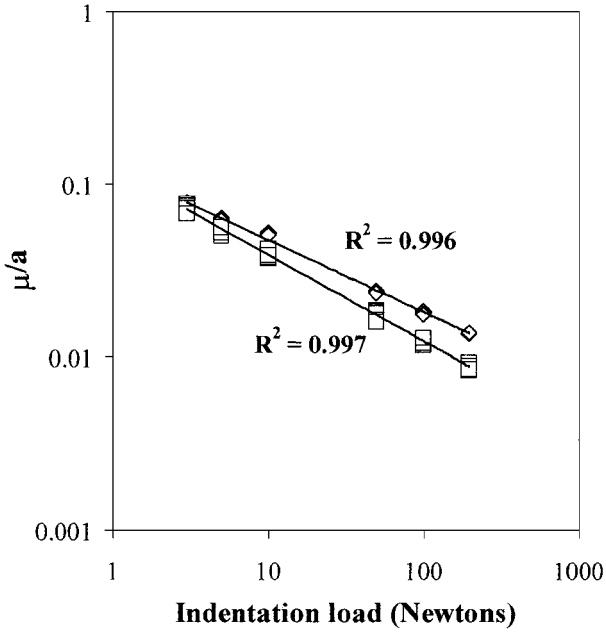

Figure 9 For Vickers indentation-induced cracks in silica coatings on BMI, the normalized mean crack spacing μ/a as a function of the indentation load. In contrast to the non-normalized crack spacing data in Fig. 8, the normalized crack spacing is described in terms of a single empirical mathematical relationship, where the straight lines indicate least-squares best fit of the data to Equation 3.

empirical expression (Fig. 9) for the normalized crack spacing, namely

$$\mu/a = \varphi P^{\varepsilon} \tag{3}$$

where $\mu =$ the mean crack spacing, $a =$ half the total crack field dimension, $P = P_{\text{app}}/P_{\text{O}} =$ normalized applied indentation load, and $P_{\text{app}} =$ applied indentation load, $P_{\text{O}} =$ a reference load.

Since there was not an obvious physically-motivated choice for reference load, P_{O} was set to 1 Newton. Thus, the prefactor φ and the exponent ε are unitless constants determined by the least-squares procedure (Table I) and the normalized value P is numerically equal to the applied indentation load P_{app} expressed in units of N. The least-squares fit to Equation 3 of the normalized crack spacing data for the unabraded coatings cured at 150°C and 175°C yield coefficients of determination, R^2, of 0.997 and 0.996 respectively. Thus, over the range of loads included in this study, Equation 3 fits the data extremely well.

Since the crack spacing data for the 175°C and the 150°C curing are described well by the same functional form (Equation 3), it was of interest to determine whether the values of the least-squares fitted constants φ and ε (Equation 3) are significantly different for the two curing conditions. To test for the statistical significance of the differences in the parameters φ and ε, we considered the standard error of estimate, S_{ee}, for each of the two constants, where S_{ee} was determined from the least-squares analysis of the crack spacing data [12, 13] (Table I). The prefactors ($\varphi_{175} = 0.1230 \pm 0.005$ and $\varphi_{150} = 0.1224 \pm 0.006$ for the 175°C and 150°C cures, respectively) differed by only 0.0006, which is about $0.1 S_{\text{ee}}(\varphi)$, where $S_{\text{ee}}(\varphi)$ is the standard error of estimate for the least-squares fitted φ values. This small difference in the φ values, compared to $S_{\text{ee}}(\varphi)$ indicates that the coefficients φ_{175} and φ_{150} are not significantly different for the 150°C and the 175°C data.

However, the ε values ($\varepsilon_{175} = -0.4153 \pm 0.0230$ and $\varepsilon_{150} = -0.4981 \pm 0.0253$ for the 175°C and 150°C cures, respectively) are apparently different, since the difference in the exponent values, $(\varepsilon_{175} - \varepsilon_{150}) \approx 4 S_{\text{ee}}(\varepsilon)$, where $S_{\text{ee}}(\varepsilon)$ is the least-squares determined standard error of estimate for ε. Although the ε values apparently vary as a function of curing conditions, it is still to be determined whether the ε values are a function of the coating/interface chemistry as well as a function of the curing temperature.

For thin, brittle films on ductile substrates, it has been observed that the nature of the coating cracking and debonding is a function of the interfacial bonding between substrate and film [14, 15]. For example, in a study of the cracking of brittle coatings on ductile fibers, Nahta and Moran [14] note competing processes between periodic cracking in the coating and debonding of the coating. A similar process involving the energy balance between debonding (spalling) and coating cracking [14] may be linked to the cracking of the silica coatings included in this study.

The apparent differences in adhesion between the silica coating and the BMI substrate as a function of curing temperature is possibly related to the curing of the SilicaFilm™. The vendor's product literature for SilicaFilm™ [16] (Emulsitone Company, Whippany, New Jersey) compares the properties of the cured SilicaFilm™ coatings with the physical properties of a "thermal oxide" (a silica layer formed when silicon is heated in air). According to the vendor [16], a SilicaFilm™ coating cured at 200°C etches in dilute HF about 1000 times faster than a thermal oxide. However, when cured at 900°C, the SilicaFilm™ coating etches in dilute HF only about three times faster than a thermal oxide, indicating a much higher chemical stability against acid attack for the coating cured at 900°C. In addition, the vendor states the SilicaFilm™ coatings cured at 800°C are about as scratch resistant as the thermal oxides, while as the curing temperature decreases, the scratch resistance of the SilicaFilm™ decreases. Of course, for the silica coatings applied in this study (all of which were fabricated from the SilicaFilm™), the curing temperature for the coating was intentionally kept well below the glass transition temperature (300°C) for the BMI substrate, thus the curing of the coatings was performed in the temperature range of 150°C–175°C. Therefore, the curing temperature restriction for the SilicaFilm™ imposed by the BMI substrates meant that the optimum chemical resistance and scratch resistance

TABLE I The prefactor φ and exponent ε obtained from the least-squares fit of the normalized mean crack spacing versus load data to Equation 3

Coating curing conditions	$\varphi \pm S_{\text{ee}}(\varphi)$*	$\varepsilon \pm S_{\text{ee}}(\varepsilon)$*
150°C/20 minutes	0.1224 ± 0.006	-0.4981 ± 0.0253
175°C/1 hour	0.1230 ± 0.005	-0.4153 ± 0.0230

* $S_{\text{ee}}(\varphi)$ and $S_{\text{ee}}(\varepsilon)$ are the standard errors of estimate for the parameters φ and ε, respectively, which are obtained from the least-squares best-fit procedure.

of the SilicaFilm^{TM} could not be realized and that the properties of the SilicaFilm^{TM} likely changed for the range of curing temperatures (150°C to 175°C) used in this experiment, since the properties of the cured films continue to change to up curing temperatures of 800°C–900°C [16]. Nevertheless, the silica films on the BMI substrates included in this study were remarkably durable, especially following the 175°C cure.

To directly determine the mechanical properties such as the elastic modulus or fracture strength of the silica films as a function of the curing temperature, one could fabricate thin film membranes of the silica film for nanoindentation testing. However, such testing is not straightforward. For thin films, if the central deflection of the film (or plate) exceeds about one-half the film thickness, then classical plate theory no longer applies and a non-linear thin plate deflection theory must be used [17, 18]. (For small deflections, one can ignore the slope of the surface to obtain linearized or classical plate theory [17], but for the large deflections, the slope of the loaded film surface can no longer be ignored and classical or linearized plate theory fails [17]).

Nanoindentation techniques employing nonlinear thin plate theory [17, 18] have been applied to determine the elastic modulus and fracture strength of a variety of thin, brittle membranes [18–21], including SiN_X [20] and polycrystalline diamond [21] films with thicknesses as small as one to two microns, which are at least comparable to the 0.2 micron thickness of the silica films used in this study. Thus, if one could fabricate thin membranes from the SilicaFilm^{TM} coatings, one might be able to directly determine mechanical property changes in the coatings as a function of the curing temperature, but a great deal of care would need to be taken in the fabrication, testing, and interpretation of the data [17–21]. Thus, the physical and chemical properties of the silica coatings produced from the SilicaFilm^{TM} may change as a function of the curing temperatures used in this experiment (150°C and 175°C), but a more complete elucidation of this point is a topic for future research.

3.4. Scatter in crack spacing for abraded coatings versus unabraded coatings

The F-test was used to compare the standard deviations of the crack spacing data for the abraded and the unabraded silica-coated BMI, where both the abraded and unabraded coatings were indented at loads of 9.8 N and 49 N. (The F-test compares the standard deviations of two data sets, such that if the F-test parameter $p < 0.05$, then the difference in standard deviations or scatter of the two data sets is said to be statistically significant [13].) The F-test comparisons for the abraded/unabraded coatings yielded p values of 0.046 for the indentations made at 9.8 N and 9.97×10^{-6} for the indentations made at 49 N. The low p values (4.6×10^{-2} and 9.97×10^{-6}) indicate that there is in fact a statistically significant difference between the standard deviations, σ_P, for the spacings in the unabraded coatings ($\sigma_{9.8} = 1.9\ \mu$m, $\sigma_{49} = 1.9\ \mu$m) compared to the standard deviation values for the abraded coatings ($\sigma_{9.8} = 1.2\ \mu$m, $\sigma_{49} = 1.0\ \mu$m).

Thus, while the abrasion did not significantly alter the mean crack spacing (as discussed in Section 3.3), coating abrasion prior to indentation reduced the scatter of the crack spacing data, as indicated by the statistically significant decrease in the scatter (standard deviation values) of the crack spacing data for abraded versus unabraded coatings. These results are analogous with the strength testing of abraded glasses, in which the scatter in the fracture strength may be reduced by abrasion since the initially random flaw population is replaced by a "controlled" flaw population [22]. The fact that there was no statistically significance change in scatter in the crack spacing data for modest changes in the applied load is also analogous to the result for strength testing of glass, where the scatter in the strength data is a relatively weak function of the applied load [22].

3.5. Changes in crack field dimensions as a function of abrasion

For a fixed Vickers indentation load, $\langle a \rangle$, the mean of half-diagonal lengths of the diamond-shaped crack regions was a factor of about 1.15 times larger for the abraded coatings than for the unabraded coatings. For the unabraded coatings indented at 9.8 N, $\langle a \rangle = 116.6$ microns, while for the abraded coatings $\langle a \rangle = 135.8$ microns, with standard deviations of 1.6 microns and 1.7 microns, respectively. Similarly, for the coatings indented at 49 N, $\langle a \rangle = 260.1$ microns for the unabraded coatings and $\langle a \rangle = 288.6$ microns for the abraded coatings, with standard deviations of 2.9 microns and 2.0 microns, respectively.

For both the 9.8 N and 49 N loads, the unabraded and abraded $\langle a \rangle$ values are separated by about 10 standard deviations, thus clearly $\langle a \rangle$ increased with abrasion. The increase in $\langle a \rangle$ is presumably due to the abrasion process introducing a flaw population of greater length than the initial flaw population, leading to coating fracture at a greater distance from the indent center.

4. Summary and conclusions

The area spalling fraction, f_S, and the mean crack spacing, μ, were the two measures of integrated coating damage selected in this study to characterize the results of the Vickers and Hertzian loading of thin silica coatings adhered to BMI substrates. This study shows that both f_S and μ can be quite sensitive to the coating curing temperature. For example, curing the silica coatings 175°C for one hour reduced the fractional spalling area, f_S, from 0.14 to 0.25 (for coatings cured at 150°C for 20 minutes) to between 0.02 to 0.05 for coatings cured at 175°C for one hour (Fig. 4). A future "fine tuning" of the curing temperature and curing time may further reduce and optimize the value of f_S. Reducing f_S is of course of critical importance for silica or other brittle coatings that may be used to protect the BMI substrates from erosion or fluid ingress.

Within a given indentation crack field, the cracks were approximately evenly (uniformly) spaced, for both Vickers and Hertzian indentations. However, the crack spacing was subject to change depending on (1) curing conditions and (2) indentation load. For coatings

cured at 150°C for 20 minutes, the mean spacing was a very weak function of the indentation load and indenter shape. In contrast, the mean crack spacing increased with indentation load for the unabraded coatings cured at 175°C for one hour (Fig. 8). However, for both sets of Vickers indentations (coatings cured at 175°C and coatings cured at 150°C) the normalized mean crack spacings, μ/a, were described very well by an empirical power law dependence on load such that $\mu/a = \varphi P^{\varepsilon}$ (Equation 3). The prefactor φ was essentially the same for the two curing conditions (175°C and 150°C) while the exponent ε was slightly different for the two curing conditions (Fig. 9).

In the future, the effect of different curing conditions on both the spalling area fraction, f_S, and the exponent, ε, in Equation 3, should be investigated further. The authors and co-workers have begun Fourier Transform Infrared studies to help understand the nature of the coating/substrate chemistry and to relate that chemistry to the cracking and spalling behavior.

Acknowledgments

The authors acknowledge Professor A. Lee and graduate student J. E. Lincoln (both of the Materials Science and Mechanics Department, Michigan State University) for supplying the BMI substrates used in this study.

References

1. E. E. SHIN, R. J. MORGAN, J. ZHOU, J. E. LINCOLN, R. J. LUREK and D. B. CURLISS, in Proceedings of the American Society for Composites, 12th Technical Conference, edited by R. F. Gibson and G. M. Newaz (Techonomic Publishing Co., Lancaster, PA, 1997) p. 1113.
2. R. J. MORGAN, R. J. JUREK, A. YEN and T. DONNELLAN, *Polymer* **34** (1993) 835.
3. R. J. MORGAN, E. E. SHIN, B. ROSENBERG and A. JUREK, *ibid.* **38** (1997) 639.
4. J. S. COLTON, *Polymer Composites* **19** (1998) 732.
5. D. E. HENDERSON and J. T. HYNES, *Advanced Materials and Processes* **136** (1989) 43.
6. C. MUKHERJEE and E. D. CASE, *J. Mater. Sci.* **35** (2000) 1389.
7. B. R. LAWN, in "Fracture Mechanics of Ceramics," Vol. 5, edited by R. C. Bradt, A. G. Evans, D. P. H. Hasselman and F. F. Lange (Plenum Press, New York, 1983) p. 1.
8. S. W. YURGARTIS, M. D. BUSH and B. E. MAST, *Surface & Coatings Technology* **70** (1994) 131.
9. S. M. ROSS, in "Introduction to Probability Models" (Academic Press, New York, 1972) p. 27.
10. D. A. BELSY, E. KUH and R. E. WELSH, in "Regression Diagnostics" (Wiley, New York, 1980) p. 19.
11. R. D. COOK and S. WEISBERG, in "Residuals and Influence in Regression" (Chapman and Hall, New York, 1982) p. 36, 54.
12. J. MANDEL, in "Statistical Analysis of Experimental Data" (Dover Publications, Inc., New York, 1964) p. 85.
13. W. VOLK, in "Statistics for Engineers" (McGraw-Hill, New York, 1958) p. 145.
14. R. NAHTA and B. MORAN, *Int. J. Fracture* **79** (1996) 351.
15. S. SHIEU and M. H. SHIAO, *Thin Solid Films* **306** (1997) 124.
16. Product literature for SilicaFilm™, Emulsitone Company, Whippany, New Jersey, 1997.
17. C. W. BERT and J. L. MARTINDALE, *AIAA J.* **26** (1988) 235.
18. C. LIU and E. D. CASE, *Exp. Mech* **37** (1997) 175.
19. *Idem., Exp. Techniques* **21** (1997) 28.
20. S. HONG, T. P. WEIHS, J. C. BRAVMAN and W. D. NIX, *J. Electronic Mat.* **19** (1990) 903.
21. W. H. GLIME, E. D. CASE, J. MATTAVI and D. K. REINHARD, in Proceedings of the American Society for Composites 8th Technical Conference on Composite Materials (Techonomic Publishing Co., Lancaster, PA, 1993) p. 921.
22. B. R. LAWN, in "Fracture of Brittle Solids," 2nd ed. (Cambridge University Press, Cambridge, England, 1993) Sections 8.2.1, 8.4.1, and 9.1.2.

Received 24 February
and accepted 23 October 2000